Ionization of Rydberg hydrogen by a half-cycle pulse

Alejandro Bugacov
Physics Department, University of Southern California, Los Angeles, California 90089-0484

Bernard Piraux
Institut de Physique, Université Catholique de Louvain, B-1348 Louvain-la-Neuve, Belgium

Marcel Pont and Robin Shakeshaft
Physics Department, University of Southern California, Los Angeles, California 90089-0484
(Received 21 September 1994)

We have calculated, by numerically integrating the time-dependent Schrödinger equation, the probability for ionization of a hydrogen atom from a high Rydberg state by a half-cycle pulse whose duration is comparable to, or shorter than, the period of the Rydberg orbit. We have chosen a pulse whose parameters are the same as the pulse used in the experiment of R. R. Jones, D. You, and P. H. Bucksbaum [Phys. Rev. Lett. **70**, 1236 (1993)]. We compare our results with the classical results and with the experimental data of Jones *et al.*, and we also present results for energy and angular distributions. Finally, we derive an approximate conservation law which applies in the limit of very short pulse times.

PACS number(s): 32.80.Rm

I. INTRODUCTION

Recently Jones, You, and Bucksbaum [1] experimentally investigated the ionization of a sodium atom in a high Rydberg state by a half-cycle linearly polarized pulse of light. Following this experiment two theoretical studies of the ionization of Rydberg hydrogen by a half-cycle pulse were reported in [2–4]. (The sodium atom, in a high Rydberg state, behaves quite similarly to hydrogen. Indeed, the validity of the hydrogenic approximation was confirmed by the classical calculations for sodium, reported on in Ref. [3].) In this paper we present the results of quantum calculations for hydrogen which support and augment the previous results. In particular, we have performed calculations for the same parameters as the experiment, i.e., we have used the same pulse (shape and duration) and the same principal quantum number for the initial state of the atom. We also present an approximate conservation law which applies in the limit of very short pulse times.

As in previous calculations [5] we represented the wave function of the electron on a *complex* Sturmian basis. The time-dependent Schrödinger equation reduces to a set of coupled first order differential equations in time. However, in contrast to Ref. [5] where we used the split-operator method to integrate these differential equations, we used an *implicit* Runge-Kutta algorithm [6] which is especially suited to parallel computation and which is both stable and accurate. This enabled us to handle a very large number of coupled differential equations; a typical basis consisted of 128 radial (Sturmian) functions per angular momentum quantum number l, with l spanning the range $0 \leq l \leq 45$.

The electric field, $\mathbf{F}(t)$, can be treated within the dipole approximation. We choose the z axis to be both the electric field polarization axis and the quantization axis and write $\mathbf{F}(t) = F(t)\hat{\mathbf{z}}$. The field relevant to the experiment can be fitted by the pulse shape [7]

$$F(t) = 0, \quad t < 0 \tag{1}$$

$$F(t) = 29.56F_0[17.75(t/\tau)^3 e^{-8.87t/\tau} - 0.412(t/\tau)^5 e^{-4.73t/\tau}], \quad t \geq 0 \tag{2}$$

where F_0 is the peak value of the electric field, which was varied, and where τ was held fixed at $\tau = 1$ psec. We considered several values of τ in our calculations, including $\tau = 1$ psec. The pulse given by Eq. (2) consists of a large half-cycle (hc) lobe of short duration, whose peak value is F_0 and whose full width at half maximum is roughly $t_{\rm hc} = 0.44\tau$. This main lobe is followed by a long but shallow tail that has opposite (negative) polarity — see Ref. [1]. The impulse communicated to the electron by the electric field over the time interval $[0, t]$ is (note that we use atomic units unless stated otherwise)

$$Q(t) = -\int_0^t dt'\, F(t'). \tag{3}$$

Assuming that no static-field component is present, the integrals over the negative tail and the positive main lobe should cancel each other to give $Q(\infty) = 0$, in accordance with the fact that within the dipole approximation photons carry no momentum. However, for the pulse shape of Eq. (2) the total time integral of the electric field does not vanish since the fit to the negative tail is inaccurate at *very large* times. This inaccuracy has no bearing on the ionization probability since at very large times the tail is too weak to ionize the atom. Moreover, in the laboratory experiment, the pulse is not a plane wave, but rather a focused pulse, and the electron will leave the focal region

long before it can experience the entire negative tail.

In the next section we discuss the impulse approximation. In Sec. III we present our numerical results and in Sec. IV we derive an approximate conservation law.

II. IMPULSE APPROXIMATION

The momentum transferred to the electron by the main (hc) lobe is

$$\Delta p_{\rm hc} = Q(t_0), \tag{4}$$

where 0 and t_0 are the end points of the main lobe. Let $p_n \equiv 1/n$ and $T_n \equiv 2\pi n^3$ be the characteristic momentum and orbital period, respectively, of the electron in the initial Rydberg orbit whose principal quantum number is n. Following Reinhold and co-workers [2,3] we introduce the scaled momentum transferred by the main lobe,

$$\Delta p_0 = \Delta p_{\rm hc}/p_n, \tag{5}$$

and the scaled duration of the main lobe,

$$T_0 = t_{\rm hc}/T_n. \tag{6}$$

(In the classical limit, the probability for ionization by the main lobe depends only on Δp_0 and T_0 [2,3].)

If the main lobe of the pulse delivers a sudden ($T_0 \ll 1$) and powerful ($\Delta p_0 \gg 1$) kick to the electron, the impulse approximation applies. This approximation amounts to neglecting the influence of the nucleus on the electron while the electron interacts with the electric field. Hence, during the time the electric field acts, the Hamiltonian can be approximated as $H_{\rm imp}(t) = Q^2(t)/2 + F(t)z$ and the evolution operator becomes, simply, $\exp[-i\int_0^t dt'\ H_{\rm imp}(t')]$. Since $\int_0^t dt'\ H_{\rm imp}(t')$ is just a spatial constant plus $Q(t)z$, the ionization probability, within the impulse approximation, is [3]

$$P_{\rm imp} = \int d^3\mathbf{k}\ |\langle\psi_{\mathbf{k}}^-|e^{iQz}|\psi_{nlm}\rangle|^2, \tag{7}$$

where $|\psi_{nlm}\rangle$ and $|\psi_{\mathbf{k}}^-\rangle$ represent the initial and final states of the electron, and where Q is the appropriate momentum transfer, i.e., we insert $Q = \Delta p_{\rm hc}$ to yield the probability for ionization by the main lobe.

We can evaluate $P_{\rm imp}$ rather easily by first rewriting Eq. (7) as

$$P_{\rm imp} = \int_0^\infty dE\ P_{\rm imp}(E), \tag{8}$$

where, with $G(E)$ the Coulomb Green's function,

$$\begin{aligned} P_{\rm imp}(E) &= \int d^3\mathbf{k}'\ \delta(k'^2/2 - E)|\langle\psi_{\mathbf{k}'}^-|e^{iQz}|\psi_{nlm}\rangle|^2, \\ &= -(1/\pi){\rm Im}\langle\psi_{nlm}|e^{-iQz}G(E)e^{iQz}|\psi_{nlm}\rangle. \end{aligned} \tag{9}$$

Using a (complex) Sturmian representation of $G(E)$ in parabolic coordinates, we were able to evaluate $P_{\rm imp}(E)$ without much computational effort.

The kick delivered to the electron by the main lobe is partially offset by the opposite kick delivered by the negative tail [i.e., Q is reduced by about 17% for the pulse form of Eq. (2)], and so within the impulse approximation the full pulse is not as effective as the main lobe in ionizing the atom. Note that in making the dipole approximation, we treat the pulse as an infinite plane wave. Hence, if the impulse approximation were applicable during the entire passage of the pulse, and if the kick delivered by the main lobe were completely offset by the reverse kick of the negative tail, no ionization would occur; from Eq. (7) we have $P_{\rm imp} = 0$ when $Q = 0$. However, in the case of a plane-wave pulse, electron scattering from the nucleus cannot be neglected during the long negative tail; indeed, the net momentum imparted to the electron must ultimately be supplied by electron scattering from the nucleus, even though the electron may not have time to scatter from the nucleus during the main lobe. Nevertheless, if the negative tail is very long and shallow it will hardly influence the ionization probability.

In reality, of course, the pulse is not an infinite plane wave, but rather a focused pulse. Therefore, the electron will leave the focal region, along the electric field axis, long before it can experience the entire negative tail. As the electron leaves the focal region it will be accelerated by the ponderomotive force, and thereby acquire momentum in addition to that imparted by the main lobe of the pulse. Consequently, if the main lobe delivers a sudden powerful impulse to the electron, the ionization probability can be accurately calculated from applying the sudden approximation to the main lobe, even though the energy and angular distributions will not be given corrrectly.

Suppose that the main lobe is indeed sudden ($T_0 \ll 1$) and powerful ($\Delta p_0 \gg 1$). If, just before being hit by the pulse, the electron has a momentum $\mathbf{p}$ and is at a distance r from the nucleus, its energy after being hit by the main lobe, i.e., after receiving an impulse $\Delta\mathbf{p}_{\rm hc}$, is $(\mathbf{p} + \Delta\mathbf{p}_{\rm hc})^2/2 - 1/r$ (the electron does not have time to move during the main lobe). Averaging over all directions of $\mathbf{p}$, and noting that $\mathbf{p}^2/2 - 1/r = -p_n^2/2$, the energy distribution of the emergent electron, immediately after the main lobe has passed, is centered at roughly $(\Delta p_{\rm hc})^2/2 - (p_n^2/2)$, i.e., at

$$E_{\rm peak} = \frac{1}{2}[(\Delta p_0)^2 - 1]p_n^2 \tag{10}$$

with a width proportional to $p_n\Delta p_{\rm hc}$. (If $\Delta p_0 < 1$ the kick is too weak for the electron to be impulsively knocked out of the atom.) The angular momentum distribution of the emergent electron, immediately after the main lobe has passed, is centered at about $r_n\Delta p_{\rm hc}$, where $r_n \equiv n^2$ is the characteristic radius of the atom in its initial Rydberg state. The electron can emerge with a linear momentum of magnitude k that is much larger than $\Delta p_{\rm hc}$ only if it is ejected from a high momentum (i.e., $|\mathbf{p}| \gg p_n$) component of the initial bound state momentum distribution $|\langle\mathbf{p}|\psi_{nlm}\rangle|^2$. However, although the angular momentum $l = kr$ increases with increasing k, the electron can have a high momentum component in the initial bound state only if it is initially at a distance r from the nucleus that is very small ($r \ll r_n$). As a

result, l decreases rapidly in the high-energy tail of the energy distribution.

Of course, as already noted, both the negative tail of the pulse (even if it is weak) and ponderomotive scattering may significantly influence the energy and angular distributions, while not affecting the ionization probability.

III. RESULTS

In Fig. 1 we show the probability for the atom to be ionized if it is initially in the $9d$ ($m = 0$) state. We show the ionization probability for different durations of the pulse, holding the scaled momentum fixed, at $\Delta p_0 = 1.9$. The solid curve is the "exact" probability for ionization by the full pulse, calculated by solving the time-dependent Schrödinger equation. The horizontal long-dashed and short-dashed lines in Fig. 1 are the ionization probabilities, calculated within the impulse approximation, for the atom to be ionized by the main lobe and by the full pulse, respectively. We see that the exact ionization probability begins to level off as T_0 approaches zero, rising above the impulse approximation result for the full pulse (since electron scattering from the nucleus mitigates the effect of the reverse kick by the negative tail), but remaining below the impulse approximation result for the main lobe (since the reverse kick by the negative tail is not eliminated entirely). In the present case, where Δp_0 is larger than unity but not much larger, the impulse approximation begins to break down as T_0 increases beyond about 0.2. If Δp_0 were much larger than unity we would expect the impulse approximation to apply up to significantly larger T_0. Incidentally, note that, since we hold $\Delta p_{\rm hc}$ fixed, F_0 decreases as T_0 increases, and for large T_0 ionization occurs through tunneling.

In Fig. 2 we show the ionization probability density in the energy-angular momentum plane at the end of the main lobe. These results were calculated by solving the time-dependent Schrödinger equation for a pulse whose peak field and duration are fixed, for the cases where the initial bound state is the 7d, 8d, or 9d states, for which $T_0 = 0.35$, 0.24, and 0.17, respectively, and $\Delta p_0 = 1.51$, 1.73, 1.94, respectively. We have indicated, by a vertical arrow, the point $E_{\rm peak}$, i.e., the center of the energy distribution as predicted in the impulse approximation — recall Eq. (10). A horizontal arrow indicates the approximate cutoff in angular momentum quantum number l (i.e., the maximum l, beyond which the population falls off rapidly). Since a discrete basis was used, the allowed energies of the electron are discrete, so the plot of the probability density is not continuous. We see a significant population of high-l states, as did LaGattuta and Lerner [4]. We also see that the most probable l decreases rapidly in the high-energy tail of the energy distribution, as discussed in Sec. II. Finally, recall that for $T_0 \ll 1$ and $\Delta p_0 \gg$ (impulse approximation) the angular momentum

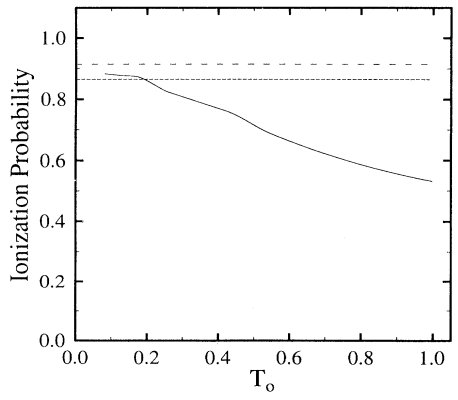

FIG. 1. Probability for ionization from the $9d$ state vs the scaled (dimensionless) pulse duration T_0 when the scaled momentum imparted to the electron is held fixed. The long-dashed and short-dashed horizontal lines are the probabilities calculated within the sudden approximation for ionization by the main lobe and the full pulse, respectively.

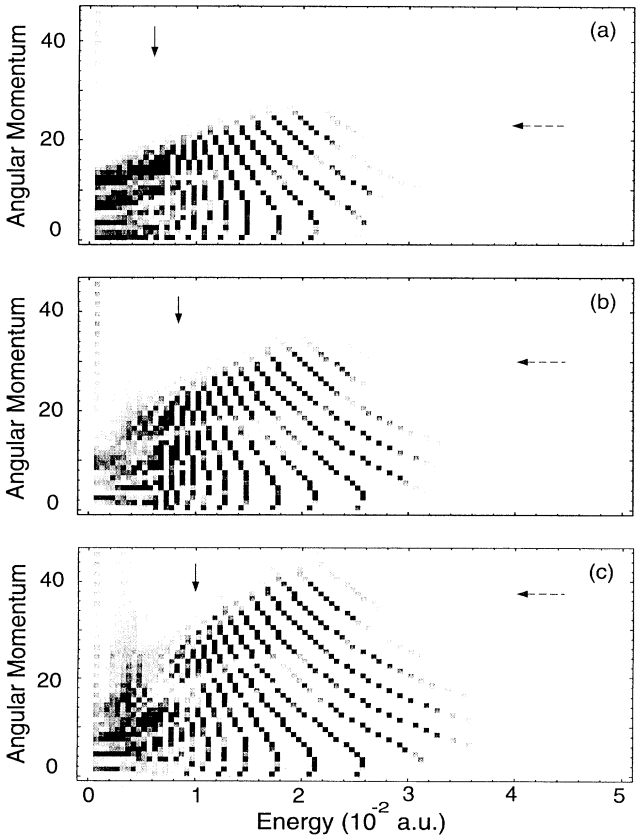

FIG. 2. Ionization probability distribution over the angular momentum quantum number and the energy of the emergent electron. Darker areas are regions of higher probability. The peak field of the pulse is fixed and the width of the main lobe is 0.018 psec. The initial bound state is (a) $7d$, (b) $8d$, and (c) $9d$. The vertical arrows mark the points at which the energy distribution should peak according to the impulse approximation — see Eq. (10) of text. The horizontal arrows mark the approximate cutoff in angular momentum.

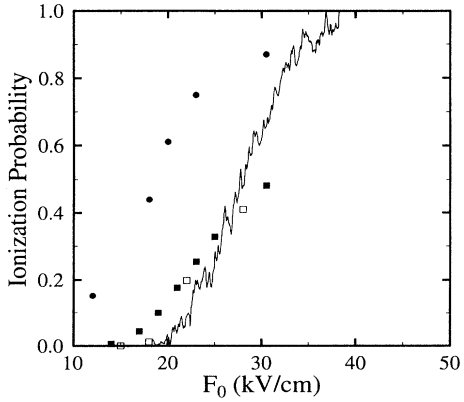

FIG. 3. Probability for ionization from the $15d$ state vs the peak field F_0. Solid line: data from the experiment of Ref. [1], with F_0 shifted by factor of 2.5, as recommended in Ref. [1]. Solid squares: present results, calculated by solving the time-dependent Schrödinger equation. Open squares: classical results from Ref. [1]. Solid circles: results calculated within the impulse approximation.

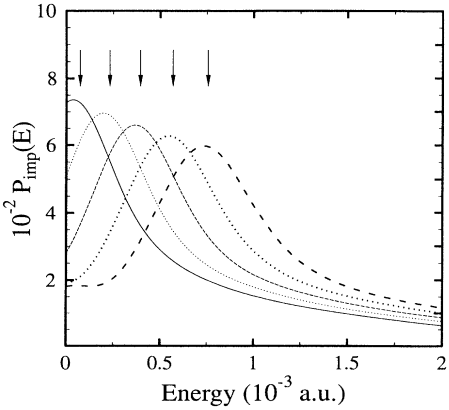

FIG. 5. Energy distribution of the electron, ejected from the $20d$ state, according to the impulse approximation. The curves correspond, from left to right, to the peak field strengths 17, 18, 19, 20, and 21 kV/cm. The arrows mark the points at which the energy distribution is centered according to Eq. (10) of the text.

distribution should be centered at roughly $r_n \Delta p_{\rm hc}$, which grows with increasing n as n^2; however, the growth in the cutoff seen in going from Fig. 2(a) to 2(b) to 2(c), while more rapid than linear, is not as rapid as n^2.

We have calculated, by solving the time-dependent Schrödinger equation, the probability for ionization from the $15d$ ($m = 0$) state by a full pulse whose main lobe has a width of 0.44 psec, the same as in the experiment of Jones *et al.* [1]. In Fig. 3 we compare the ionization probability with the experimental data, and with the results of the classical calculations of Jones *et al.* [1], for various peak field strengths. Our quantum results agree well with the classical results, and the agreement with experimental data is also fairly good up to the highest field strength we could handle. (Our calculations are limited primarily by the basis size required for convergence; as the peak field strength F_0 increases, the required basis size increases even more rapidly.) We also show in Fig. 3 the results calculated using the impulse approximation for the probability of ionization *by the main lobe*, but the agreement with the impulse approximation is poor, which is perhaps expected since T_0 is not small, i.e., $T_0 = 0.9$. However, Jones *et al.* [1] also measured the probability for ionization from the $20d$ and $35d$ ($m = 0$) states, for which $T_0 = 0.4$ and 0.07, respectively. The impulse approximation should be more accurate for these higher n states, and that is confirmed by Fig. 4, where we compare our impulse approximation results (for ionization by the main lobe) with the experimental data and with the classical calculation results of Jones *et al.* for ionization from the $20d$ state. We have not carried out full calculations for the $20d$ state since they would be expensive (a very large basis would be required) and we would not expect to obtain results much different from those found using the impulse approximation, in contrast to the case of the $15d$ state. In Fig. 5 we show results (obtained from the impulse approximation) for the energy distribution $P_{\rm imp}(E)$ of the electron at the end of the main lobe, for different peak field strengths, when the atom is initially in the $20d$ state. The arrows mark the energies $E_{\rm peak}$ at which the energy distribution should peak according to Eq. (10).

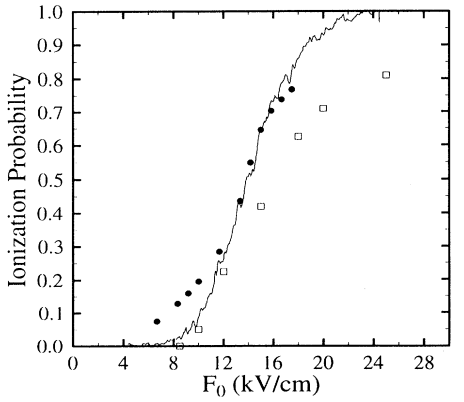

FIG. 4. Probability for ionization from the $20d$ state, for the same pulse as in Fig. 3. Solid line: data from experiment of Ref. [1]. Open squares: results calculated from classical calculations of Ref. [1]. Solid circles: results calculated within the impulse approximation.

IV. CONSERVATION LAW

The pure hydrogen atom, or, more generally a hydrogenlike ion with atomic number Z, has a special constant of motion, the Runge-Lenz vector. Redmond [8] pointed out that in the presence of a static electric field, $\mathbf{F}$, the hydrogenlike ion retains a special symmetry, and he showed

that $\mathbf{F}\cdot\mathbf{C}(\mathbf{F},\mathbf{p})$ is constant of motion, where $\mathbf{C}(\mathbf{F},\mathbf{p})$ is a generalization of the Runge-Lenz vector

$$\mathbf{C}(\mathbf{F},\mathbf{p}) = \hat{\mathbf{r}} + \frac{1}{2Z}(\mathbf{L}\times\mathbf{p} - \mathbf{p}\times\mathbf{L}) - \frac{1}{2Z}(\mathbf{r}\times\mathbf{F})\times\mathbf{r}, \tag{11}$$

where $\mathbf{r}$, $\mathbf{L}(=\mathbf{r}\times\mathbf{p})$, and $\mathbf{p}$ are the coordinate relative to the nucleus, the orbital angular momentum, and the canonical momentum, respectively, of the electron.

When a system is subject to a sudden perturbation, the time-evolution operator can often be accurately represented by the first one or two terms of the Magnus expansion [9]. The present system of interest is a hydrogenlike ion, whose Hamiltonian is $H_a \equiv (\mathbf{p}^2/2) - Z/r$, subject to an interaction $\mathbf{F}(t)\cdot\mathbf{r}$ with a pulse of short duration T. Retaining the first two terms in the Magnus expansion amounts to replacing the true time-dependent Hamiltonian $H(t) = H_a + \mathbf{F}(t)\cdot\mathbf{r}$ over the time interval $0 < t < T$ by the effective time-independent Hamiltonian

$$H_{\text{eff}} = \frac{1}{T}\int_0^T dt_1\, H(t_1) - \frac{i}{2T}\int_0^T dt_1 \int_0^{t_1} dt_2\, [H(t_1), H(t_2)]. \tag{12}$$

The impulse approximation, used in the preceding sections, can be recovered by neglecting the Coulomb potential $-Z/r$ and putting $\mathbf{p} = \mathbf{Q}(t)$ in $H(t)$. (With these replacements the commutator vanishes, so all terms but the first vanish in the Magnus expansion.) Evaluating the commutator, and performing the time integration in Eq. (12) yields

$$H_{\text{eff}} = H_a + \mathbf{F}_{\text{av}}\cdot\mathbf{r} + (1/c)\mathbf{A}_{\text{eff}}\cdot\mathbf{p}, \tag{13}$$

where $\mathbf{F}_{\text{av}}$ is the average electric field, given as

$$\mathbf{F}_{\text{av}} = \frac{1}{T}\int_0^T dt\, \mathbf{F}(t), \tag{14}$$

and where $\mathbf{A}_{\text{eff}}$ is an effective vector potential given by

$$\mathbf{A}_{\text{eff}} = -\frac{c}{2T}\int_0^T dt_1 \int_0^{t_1} dt_2\, [\mathbf{F}(t_2) - \mathbf{F}(t_1)]. \tag{15}$$

Now the first two terms on the right-hand side of Eq. (13) constitute the Hamiltonian of a hydrogenlike atom in a static electric field $\mathbf{F}_{\text{av}}$, for which Redmond derived a constant of motion. However, we can absorb the third term into the canonical momentum since

$$H_{\text{eff}} = e^{-i\mathbf{a}\cdot\mathbf{r}}(H_a + \mathbf{F}_{\text{av}}\cdot\mathbf{r})e^{i\mathbf{a}\cdot\mathbf{r}} - \mathbf{a}^2/2, \tag{16}$$

where $\mathbf{a}$ is the spatial constant

$$\mathbf{a} = -(1/c)\mathbf{A}_{\text{eff}}. \tag{17}$$

Writing $\mathbf{P} = \mathbf{p} + \mathbf{a}$, and $\mathbf{L} = \mathbf{r}\times\mathbf{P}$, it follows that $\mathbf{F}_{\text{av}}\cdot\mathbf{C}(\mathbf{F}_{\text{av}},\mathbf{P})$ has approximately the same values at the beginning and at the end of the pulse. However, we must stress that this conservation law is accurate only if the Hamiltonian of Eq. (13) (which is separable in parabolic coordinates) accurately describes the influence of the pulse on the dynamical motion of the electron; we require, in particular, that the last term on the right-hand side of Eq. (13) be a small correction to the second term.

In the case of a "one"-electron alkali atom, whose core potential is nonhydrogenic, the energy levels within a Rydberg manifold are not degenerate. However, provided that adjacent Rydberg manifolds do not overlap, which is true when the magnetic quantum number m is sufficiently large, this nondegeneracy will not be apparent over a time interval short compared to $1/\Delta E$, where ΔE characterizes the magnitude of the nondegeneracy. Therefore, at least for the $m > 1$ states, we expect the conservation law to hold as long as the pulse duration is short compared to $1/\Delta E$.

ACKNOWLEDGMENTS

We thank Professor W. E. Cooke for several helpful comments. This work was supported by the National Science Foundation under Grant No. PHY9315704, and by the National Center for Supercomputing Applications under Grant No. PHY940011N; we utilized the Connection Machine Model-5 at the National Center for Supercomputing Applications, University of Illinois at Urbana-Champaign. One of us (B.P.) was supported in Belgium by the Fonds National de la Recherche Scientifique.

[1] R. R. Jones, D. You, and P. H. Bucksbaum, Phys. Rev. Lett. **70**, 1236 (1993).
[2] C. O. Reinhold, M. Melles, and J. Burgdörfer, Phys. Rev. Lett. **70**, 4026 (1993).
[3] C. O. Reinhold, M. Melles, H. Shao, and J. Burgdörfer, J. Phys. B **26**, L659 (1993).
[4] K. J. LaGattuta and P. B. Lerner, Phys. Rev. A **49**, R1547 (1994).
[5] M. Pont, D. Proulx, and R. Shakeshaft, Phys. Rev. A **44**, 4486 (1991).
[6] See, e.g., L. Lapidus and J. H. Seinfeld, *Numerical Solution of Ordinary Differential Equations*, Vol. 74 of *Mathematics in Science and Engineering*, edited by R. Bellman (Academic, New York, 1971).
[7] R. R. Jones (private communication).
[8] P. Redmond, Phys. Rev. **133**, B1352 (1963).
[9] W. Magnus, Commun. Pure Appl. Math. **7**, 649 (1954).